Chapter 3

Mechanical Excitation via Pulsed Laser Ablation

The mechanical excitation of a granular system can be achieved by applying a controlled force or momentum vector to one or more parts of the granular system. Knowing and controlling the applied force, or initial velocity, are the starting points for numerical, theoretical, and experimental investigation of the system. Conventional means to mechanically excite a macroscopic granular system include using collision with a particle at controlled momentum [125] or actuating the system with a piezo transducer [16]. However, both of these methods rely on making physical contact with individual particles in the system. For example, experimentalists use collisions of freely moving particles to deliver momentum on target particles in granular systems. The freely moving particles (i.e., the strikers) need to be accelerated under a given potential before interacting with the granular system in order to reach a predetermined initial velocity. Fine aiming and precise control of the trajectory requires the accurate holding and releasing of the strikers in the potential field. For macroscopic particles, holding and releasing strikers from their initial position can be achieved by solenoids [132] or electromagnets [133]. In these cases, after being released the striker particles move along a predesigned path and apply initial conditions to the granular systems via collisions.

Achieving such controlled initial conditions at the micro-scale, however, is experimentally challenging, especially when adhesion forces can exceed the weight of the micro-particles. Adhesion forces (such as Van der Waals) and capillary forces both alter the trajectory of the strikers and therefore affect the collisions between the strikers and the target particles. The interaction between particles depends heavily on the particles' surface quality, which can degrade over time and must be monitored in real time. Therefore, a real-time verification of surface qualities, contact points, and particles' geometries is essential for the mechanical excitation of micro-granular systems. To create an experimental setup that can impart repeatable and controllable initial conditions to a micro-scale granular system, it is important to monitor the particles' geometries, the surface conditions of the contact area, and the adhesion properties of the particles with their substrate.

Pulsed laser ablation (PLA) is a process that is used widely in industry for material removal [134]. Ni et al. recently showed that PLA can be applied to generate solitary waves within macro-scale granular chains [135]. By vaporizing a controlled amount of water deposit on the surface of macro-scale particles, mechanical stress is created at one end of granular chains, which in turn generates traveling solitary waves within the chain.

In our work, we use PLA as a tool to deliver controlled momentum to a micro-scale granular system. By shining a focused laser radiation on the surface of a selected micro-particle in the system, we deliver momentum to that micro-particle, which then accelerates and acquires a controlled velocity before striking other target particles. In order to use PLA as a reliable tool for exciting micro-scale granular systems, we need to be able to predict the magnitude, as well as the direction and the variation of the striker's velocity. In the first section of this chapter, we review the history and background theory of pulsed laser ablation. In the second section, we examine the ablation process on micro-particles that are made of two different materials. We investigate the energy and directional stability of the ablation process as a tool for exciting dry micro-particles in air. In the third section, we investigate PLA as a means to excite colloidal particles in fluid. We summarize the advantages of the PLA method in the fourth section. The knowledge gained in this chapter lays the groundwork for the mechanical excitation and experimental study of dry and wet micro-particle systems in one- and two-dimensional configurations.

3.1. Theory of laser ablation for nanosecond lasers

When laser radiation is shined onto a metal's surface, the laser interacts with the electrons in the metal via inverse Bremsstrahlung scattering. The heated electrons couple with the lattice and raise the temperature locally. If the temperature exceeds the melting or boiling point of the material, the lattice is destroyed and material is ejected from the surface. If the attenuation of radiation is much slower than the electron relaxation time, we can describe the heating of the metal surface with a diffusion equation [136],

$$\mathrm{C}\frac{\partial T(z,t)}{\partial t} - \mathrm{k}\frac{\partial^2 \mathrm{T}(z,t)}{\partial z^2} = I(z,t). \tag{3.1}$$

Here, $I(z,t) = I_0(t)\,\mathrm{A}\exp(-\alpha z)$ is the laser radiation at depth z and time t that propagates within the material. Furthermore, $I_0(t)$ is the intensity of free space laser pulse input, A is the transmission of the metal surface, and α is the skin depth of the electromagnetic field in the material. In this

equation, the radiation impinges on the surface of the material ($z = 0$) and results in a temperature rise near the surface.

When the radiation is a pulsed laser, we set $I_0(t) \propto \exp(-t^2/{\tau_L}^2)$, where τ_L is the pulse width of the laser. For a sufficiently short pulse width, the temperature field can accumulate near the material surface to form a high temperature layer before there is enough time for the temperature to diffuse. Two competing factors determine the thickness of the high temperature layer on the surface, namely the heat diffusion length, $\sqrt{k\tau_L/C}$, and the skin depth of the laser within the metal, $1/\alpha$.

The energy density per unit mass within the surface is $I\ \tau_l/\rho l$, where $l = \max(\sqrt{k\tau_L/C}, 1/\alpha)$ is the thickness of the high temperature layer and ρ is the material density. In our system, the skin depth of the Nd:Yag laser radiation on stainless steel is expected to be ~2 nm, while the heat diffusion length is ~150 nm; the thickness of the high temperature layer is hence determined by heat diffusion. Ablation of material occurs when the energy density within this layer is higher than the enthalpy of evaporation, Ω. Therefore the threshold for the laser energy of ablation is

$$\frac{I\tau_L}{\rho l} > \Omega. \tag{3.2}$$

This simple model [137] explains the origins of the surface vaporization.

Now let us return to our original goal of delivering momentum to micro-particles. When ablation occurs at the surface of the material, the vaporized mass can eject at a ballistic speed of 10^4 to 10^5 m/s and the reaction force shall push the particle in the opposite direction of the momentum of the vaporized mass. In reality, the ablation process is a very complicated thermal dynamic possibility of using PLA as a reliable tool for exciting mechanical motion in micro-granular systems. To simplify this discussion, we estimate the momentum gained by a particle from the local ablation of its surface to be:

$$p_{gain} = m_{removed} v_{vapor} \propto \frac{I\tau_L}{\rho l \Omega} A_L \sqrt{\frac{T_{vapor}}{m}} \propto \frac{E_L}{\rho l \Omega} \sqrt{\frac{T_{vapor}}{m}} \propto \frac{E_L}{\rho \Omega} \sqrt{\frac{C}{k\tau_L}} \sqrt{\frac{T_{vapor}}{m}}, \tag{3.3}$$

where E_L and A_L are respectively the pulse energy and beam area of the laser. The above equation says that the momentum gained by the illuminated particle is affected by the thermal conductivity k of the material. Large thermal conductivity implies a fast heat removal from the surface layer into the

bulk material of the particle and reduces the amount of the vaporized surface materials. The momentum gained by the striker particle using PLA is proportional to the pulse energy of the laser. This is shown experimentally in the next section. It is worth mentioning that the momentum of the laser photons plays no role in this scenario.

3.2. Pulsed laser ablation on stainless steel micro-particles

In this section, we experimentally describe PLA effects on steel micro-particles in air. We placed a steel micro-particle on top of a v-shaped groove (see Fig. 2.3 above) and excited it with the laser. Figure 3.1 shows high-speed images obtained when a single particle positioned in the v-shaped groove is excited by the laser pulse. In this acquisition, the high-speed camera was operated at 1,000 fps with an exposure time of 990 µs. The first image was taken before the laser pulse was fired, and the second image (0 ms) was taken less than one microsecond after the laser pulse interacted with the particle. The presence of material ejected from the particle's surface is evident from the plume trailing the particle. Damage to the surface of the particle, which is identifiable by changes in the particle's surface texture, can be seen 1 ms after triggering the laser and then again after 8 ms. The disappearance and reappearance of the damaged surface indicates that the particle was rolling in the groove after being excited. These results indicate that PLA can excite mechanical motion of the micro-particles. Following this preliminary confirmation, we studied the fundamental mechanisms to control the momentum of the target particle and identified the essential controlling factors that influence this process.

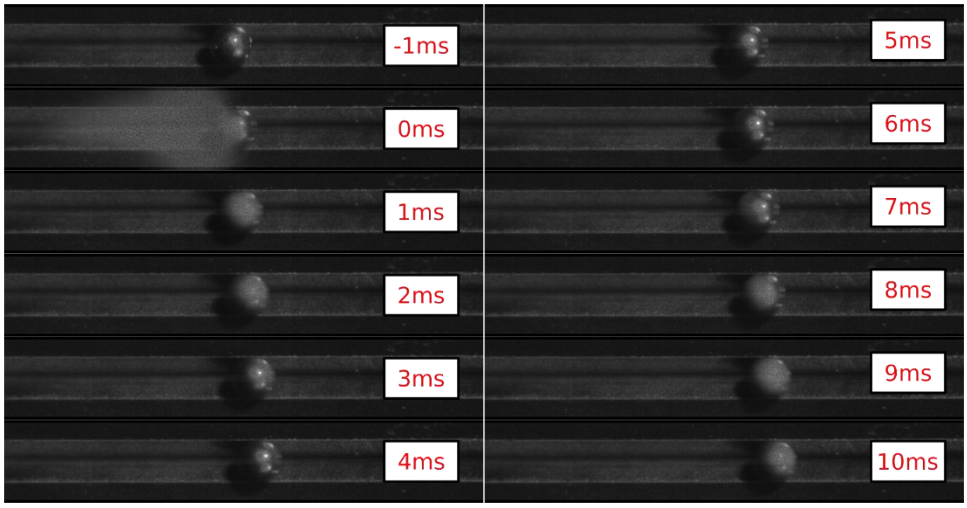

Figure 3.1: High-speed images of a micro-particle (114 µm radius, stainless steel 440c) on a v-shaped groove being illuminated by a pulsed laser at t=0 ms. Ejected materials can be seen at t=0 ms and

the damage on the particle's surface can be seen at t=1 ms and 9 ms. The sequential reappearance of the damaged surface indicates that the particle is rolling after being excited.

We performed experiments to determine the relation between the laser energy input and the momentum gained by the targeted particle. We placed target particles at a fixed location on top of the v-shaped groove and illuminated them with the pulsed laser, using pulse energy that varied between 0 to 0.8 mJ (Fig. 3.2a). The particle motion that resulted was recorded using the high-speed camera system. The speed of the particle was then obtained using image processing techniques, as described in detail in Chapter 2. The results obtained (Fig. 3.2b) show that the momentum transferred to the particles is proportional to the pulse energy, which agrees with the simple estimation derived in Eq. (3.3). We further compared the response of target micro-particles made with two different steel materials (stainless steel 316 and 440c) that do not have the same nominal thermal conductivity values. In Fig. 3.2b, it can be seen that the 316 particles gain almost twice the momentum that the 440c particles do, at the same laser energy input.

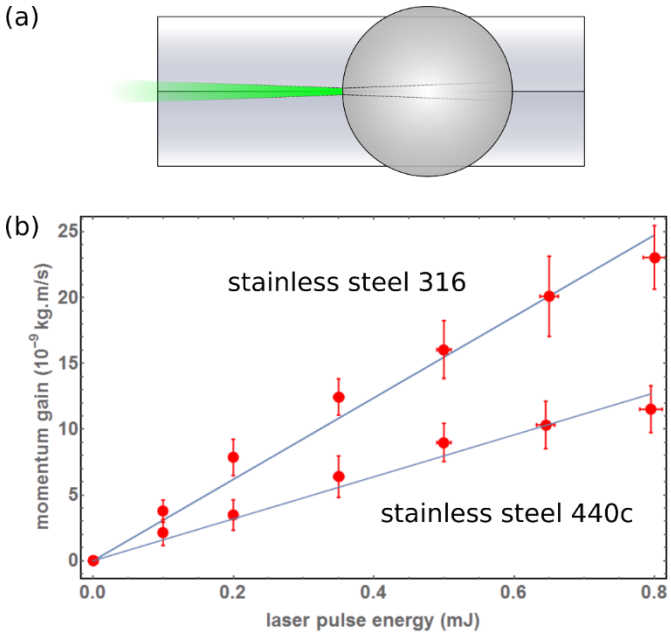

Figure 3.2: (a) Experimental scheme of calibrating the dependency of the transferred momentum to the laser pulse energy. (b) Momentum obtained by particles of two different materials (stainless steel 316 and 440c) at different laser inputs.

This difference in momentum gain indicates that the stainless steel 316 particles are more easily excited by laser ablation than the 440c particles. This result is not surprising; considering that stainless steel 316 has a smaller thermal conductivity (16.3 W/mK) than the 440c (24.2 W/mK), we expect the PLA efficiency to be higher in relation to stainless steel 440c (see the discussion in the previous section). However, experimental calibration is still required to ascertain if PLA excitation would be effective on particles of different materials, since an accurate theoretical estimation of the PLA efficiency remains difficult.

In the above experiments, when the striker particles were illuminated with the highest laser energy (0.8 mJ), the depth of the ablated mass was estimated to be ~150 nm using the data in [138]. This corresponds to only 0.01% of the mass of the test particles. As such, we considered the total mass of the excited particles as a constant. The total kinetic energy of the ejected mass and the particle was estimated to be 0.07 mJ; this is reasonable compared to the energy of the input laser pulse (0.8 mJ), if we consider that a large portion of laser is lost due to the reflection of metal surface.

3.2.1. Accuracy and repeatability

Before we can apply PLA as a tool of mechanical excitation in our micro-particles, we need to answer two main questions: (i) How repeatable is the PLA method for accelerating micro-particles?; and (ii) How accurately do we have to align the laser in order to obtain reproducible results? We conducted two tests to investigate the stability of a particle's excitation as a function of the laser's direction (Fig. 3.3a) and the position of the laser beam on the particle's surface (Fig. 3.3b). We first excited the particle with the laser beam intentionally shifted away from the center of the particle's mass by a distance x and measured the direction θ of the particle's displacement and velocity. Since the light wave front arrives simultaneously at every point of the illuminated area of the target particle (compared to the time scale of heat diffusion), we expect that the direction of the momentum gain does not depend on the direction of the beam, but only on the location of the laser beam on the surface of the particle. An offset of x should therefore lead to $\theta = \sin^{-1}(x/R)$, where R is the radius of the particle. We performed experiments to verify this assumption. We placed target particles on a clean, flat silicon wafer (instead of a groove) to allow them to move freely on a plane. Then we fixed the laser power to a specific value, to accelerate the particle to a velocity of 0.05 m/s (a relatively high speed at these scales was chosen in order to minimize the influence of the substrate's adhesion on the particle's motion). We used the micro-scope imaging system and the computer-controlled stage to locate the particles and aim the laser beam on their surfaces. In Fig. 3.3c, we plot the measured

particles' directions (red dots with error bars) and the theoretical predictions as obtained with $\theta = \sin^{-1}(x/R)$ (blue line). From the data we can see that when $x < 0.1R$, the maximum deviation is about 5°. We expect that an angular accuracy of 3° is possible when aiming the laser beam at the particles with a spatial accuracy of 10 μm (as in our experimental setup).

We performed experiments to determine the role of particle position with respect to the laser focal plane (Fig. 3.3b). The simpler estimation of the PLA efficiency in transferring momentum to target particles only depends on the laser energy. However, if the laser beam intensity diverges when it reaches the particle's surface, more energy is needed to raise the local temperature to the vaporization point. This effect is expected to lower the efficiency of the PLA process. We performed experiments to monitor variations of the target particle velocity as a function of its distance from the laser focal point. For these experiments, we used steel 440c particles positioned in a v-groove. To perform the experiments, we first used a micro-manipulator to position the target particles at the laser's focal point and then illuminated the particles and measured their velocity. We then repeated these measurements, using a computer-controlled sample stage to move the particle systematically away from the focal point by shifting its position along the reference axis (z). The results are shown in Fig. 3.3d. We can see that the momentum gain is quite stable when the laser beam is focused within $1R$ from the surface of the particles. This agrees well with our laser beam waist of 15 μm (the corresponding Rayleigh length is 1.3 mm).

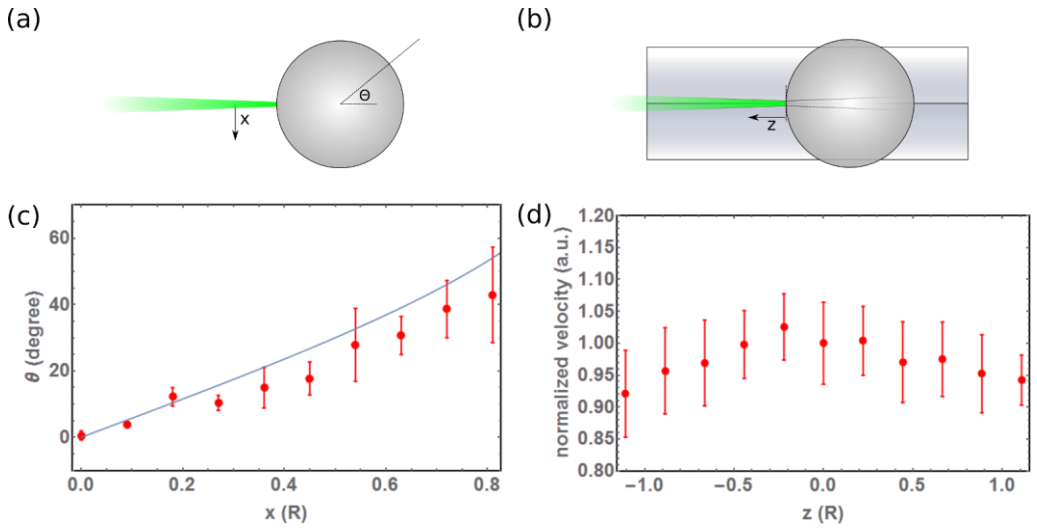

Figure 3.3: Repeatability of the laser ablation method to excite particles on a substrate. (a,b) Experimental diagrams. (a,c) Schematic diagram and results of the experiment measuring the angular dependency of the momentum to the off axis distance. (b,d)

Schematic diagram and results of the experiment measuring the accuracy requirement for particles along the optical axis of the laser. A 15% variation of output velocity is observed.

However, a closer examination of Figs. 3.2 and 3.3 reveals a velocity variation of ~15% in all data, which is a limitation of our experimental system. Such velocity variation can arise from imperfections in the stainless steel particles, from the energy stability of the laser (about 1% in our system), from the angular stability of the laser beam, or other systematic errors. We conclude that under realistic operation conditions, our laser system can deliver momentum to our stainless steel micro-particles with 15% accuracy in magnitude and 3% angular stability. In the next section, we investigate the laser energy transfer to silica colloids that are immersed in water, which are used in the dynamic testing of two-dimensional colloidal systems (as described in Chapter 6).

3.3. Pulsed laser ablation on silicon dioxide colloids

In this section, we describe the laser ablation process acting on micro-scale SiO_2 particles in fluid. As SiO_2 is a transparent dielectric material with a refractive index of 1.42, when the particles are immersed in water (refractive index of 1.33), a focused laser beam passing through the particles will be slightly diffracted by the spheres and not absorbed. In order to increase the efficiency of laser interaction, some particles are coated first with 5 nm of Cr as an adhesion layer and then with 50 nm of Au before being mixed with the uncoated particles. As the skin depth of our Nd:Yag laser beam on Au is 3 nm, we expect a very strong absorption of the laser beam in the gold layer.

We inject the coated and uncoated particles with DI water to the micro-fluidic cell. We focus the laser beam within the water on the particles, especially those that are coated. In Fig. 3.4abc, we show images of the excitation process of micro-particles in water that are taken at 45553 frames per second. The coated target particle, which is initially at rest on the micro-fluid cell, is marked by the white arrow. The laser radiation that results when we shine a laser pulse on this particle can be seen in the photo (Fig. 3.4b). After the particle is shot, we observe that the particle is relocated in the next frame and that the material ejected from the particle is left at the original location (as marked by a hollow arrow in Fig. 3.4c). This is because the high-speed camera does not directly resolve the velocity of the particle due to insufficient acquisition speed. To estimate the momentum gain of the particle at different laser power, we consider the particles are experiencing a Stokes' drag force in the background liquid, $f = -6\pi\mu Rv$, where μ is the viscosity of the liquid and R and v are respectively the radius and velocity of the particle. We can solve the relationship between the initial velocity of

the motion, v_0, and the final displacement using $\Delta x = v_0/6\pi\mu R$. By measuring the final displacement of micro-particles in a liquid with known viscosity, we can therefore calculate the initial velocity at a given laser energy. In our system, the laser beam is focused with an objective lens and expected to have a beam diameter of 10 μm. Since the laser spot is bigger than our micro-particles, the absorbed laser energy is estimated by the product of laser intensity and the area of particles.

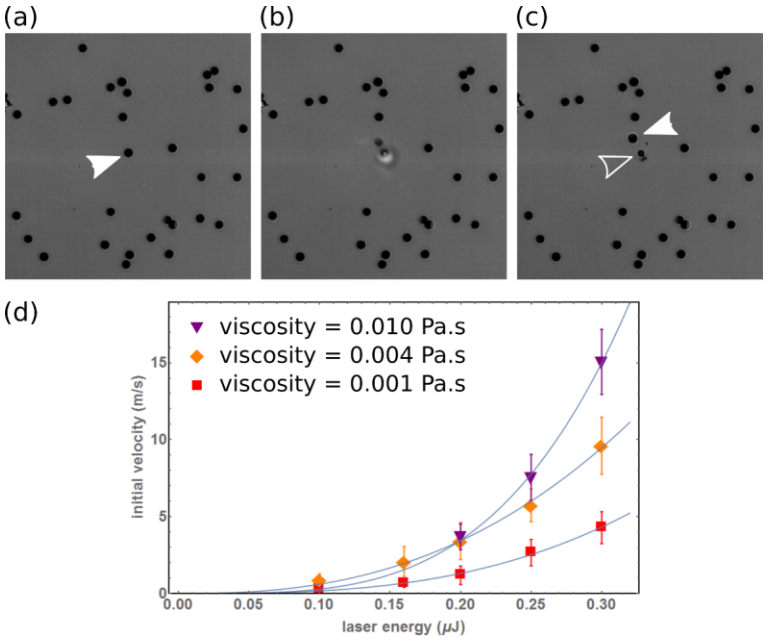

Figure 3.4: Excitation of micro-colloids' motion in water. We focus the laser on the micro-colloids in liquid. (a) The target particle (marked with a white arrow) before the laser is shone on it. (b) During the laser excitation, the laser radiation can be seen at the original position of the target particle. (c) The target particle is relocated to a new position (again marked with a white arrow). A residue of ejected dark metal flake is left at this particle's original position (marked by a hollow arrow). (d) The measured initial velocity at different laser energy and different viscosity of the background fluid.

We measure particle velocity gain due to the PLA process at varying laser energy and varying viscosity. To change the viscosity of the background fluid, we mix the water-glycerol ratio to adjust the dynamic viscosity of the background fluid from 0.001 to 0.01 Pl [139, 140]. The resultant velocity is shown in Fig. 3.4d. Here we also see the dependency of the particle velocity at different laser energy and the viscosity of background fluid, which interestingly suggests that a thicker background fluid can enhance the momentum that is gained through the PLA process. The higher the viscosity, the greater the velocity gain. We fit these data with power law $v \propto E^n$ and obtain n equals to 2.23, 2.10,

and 5.83 for dynamic viscosity equals to 0.001, 0.004, 0.01 Pl, respectively. This behavior deviates from the prediction given by Eq. (3.3), which indicates that the working principle of this wet particle excitation is very different from that of the dry particle case. The efficiency of this process (i.e., the ratio between the kinetic energy that is obtained by the micro-particle and the laser pulse energy) is about 0.001%, which is significantly lower than the efficiency in dry particle cases. With this calibration results, we can predict the momentum gain of the target particle at controlled laser energy in the background fluid that was tested.

Finally, it should be clearly stated that the particle manipulation we performed in this section is unrelated to optical tweezing [141, 142], which is a technique for manipulating micro-particles in liquid. The optical tweezer manipulates micro-particles by creating an attractive potential well to the electric dipole of the target particles by properly tuning the laser intensity and frequency. However, the process is four orders of magnitude weaker than laser ablation in our system and is omitted throughout our discussion.

3.4. Summary

In this chapter we investigated the use of pulse laser ablation as a tool for mechanically exciting dry (stainless steel particles of a radius 150 μm) and wet (SiO_2 colloids with a radius of 3.69 μm) micro-particles. For the dry particles, we measured variations of the magnitude and direction of the momentum gain as a function of the laser position and alignment. We showed that our system can deliver momentum to target stainless steel micro-particles with 15% accuracy in magnitude and 3% angular stability under realistic operation conditions. For the wet particles, we measured the velocity gains of micro-particles in fluid due to PLA at varying laser energy and at varying viscosity. The velocity gains are shown to be dependent on the viscosity of the background fluid, which indicates the interplay of the hydrodynamic system within the PLA process.

We obtained the calibration relationship between the laser energy and the momentum gained during the PLA process for both the dry and wet particles. The ability to predict the magnitude and direction of the delivered momentum is especially useful in our experiments, where direct measurements of the applied stress by direct physical contact are difficult to obtain. The laser system can deliver fast, repeatable, and automatic mechanical excitations to any point of the system that can be reached by the laser radiation. The non-contact nature of the PLA excitation system makes our experimental

apparatus also ideal for testing different micro-particle types and geometries, because the assembly and excitation of the system constitute independent parts of the setup.